



## The Influence of Polylactide Addition to The Performance of $\text{LiFePO}_4/\text{C}$ Composite as Cathode Materials

Indra Gunawan<sup>\*1</sup>, Deswita<sup>2</sup>, Heri Jodi<sup>3</sup>, Wahyudianingsih<sup>4</sup>

<sup>1,2,4</sup> Research Center for Radiation Detection and Nuclear Analysis Technology, National Research and Innovation Agency, Serpong, Indonesia

<sup>3</sup> Research Center for Advanced Materials, National Research and Innovation Agency

\*Corresponding author

E-mail: [irgun.ig@gmail.com](mailto:irgun.ig@gmail.com)

**Abstract.** The polylactide and carbon addition to  $\text{LiFePO}_4$  have been studied to investigate the behavior of  $\text{LiFePO}_4/\text{C}$  composite. The cathode material of  $\text{LiFePO}_4$  was prepared by coprecipitation of  $\text{LiOH}\cdot\text{H}_2\text{O}$ ,  $(\text{NH}_4)_2\text{HPO}_4$  and  $\text{FeSO}_4\cdot 7\text{H}_2\text{O}$  solution. The resulting  $\text{LiFePO}_4$  was mixed with biodegradable polymer PLA in the concentration of 6, 8, 10, 12 % weight of polymer. Heat treatment was done by heating the precursor at  $700^\circ\text{C}$  for 4 hour. The physical chemistry properties of cathode materials analyzed by using Simultaneous Thermal Analysis (STA), X-Ray Diffractometer (XRD), Scanning Electron Microscope (SEM), and Particle Size Analyzer (PSA) methods. High Precision LCR-meter was used to perform conductivity measurement, in which the  $\text{LiFePO}_4/\text{C}$  powder samples were prepared by using  $200\text{ kg/cm}^2$  hydrolic press. TG analysis inform gradually weight decrease at  $\text{LiFePO}_4$  temperature formation of  $470^\circ\text{C}$  and pyrolysis of remaining PLA occur at  $600^\circ\text{C}$ . From all samples XRD data indicate pure phase of  $\text{LiFePO}_4$ . SEM image shows the uniform distribution particle of sample with 6 % PLA content with conductivity of  $1.99 \times 10^{-2}\text{ Scm}^{-1}$ .

**Keywords:** coprecipitation method;  $\text{LiFePO}_4$ ; PLA; composite; physical chemistry characterization.

### 1. Introduction

Rechargeable lithium batteries are being developed for portable power applications such as electric vehicles, partly because of their high specific energies in the range 100–150 Whr/kg and theoretical specific energies in the range 425–890 Whr/kg. In recent years, olivine  $\text{LiFePO}_4$  is very extensively studied as a cathode material for Li-ion batteries because of its high theoretical capacity (170 mAh/g), stable, cheap and environmentally friendly. However, the poor level of performance has limited its application. The main factor for the poor level of performance is the capability associated with poor intrinsic electronic conductivity [1]. The behavior of  $\text{LiFePO}_4/\text{C}$  composites depends on the phase purity of the active ingredient, particle size, additive carbon structure, total carbon content, form of carbon contact and mixing and sintering recipe. [2]. Phospho-olivine type  $\text{LiFePO}_4$  has a P-O-Fe structure linkage which results in a  $\text{Fe}^{3+}/\text{Fe}^{2+}$  redox reaction with an energy of 3.4 V compared to  $\text{Li}/\text{Li}^+$ .  $\text{LiFePO}_4$  has a three-dimensional structure that contains pathways

Received February 24, 2023; Accepted March 17, 2023; Published March 31, 2023

<https://doi.org/10.55043/jfpc.v2i1.72>

This is an open access article under the CC BY-SA 4.0 license <https://creativecommons.org/licenses/by-sa/4.0>

for lithium ions, but has a high reversible current density capacity so that there is a loss in current density. This high discharging inability to  $\text{LiFePO}_4$  is associated with low electronic conductivity and slow  $\text{Li}^+$  diffusion at the interface [3]. Diffusion of  $\text{Li}^+$  at the  $\text{LiFePO}_4/\text{FePO}_4$  interface, causes the concentration of  $\text{Li}^+$  moving through the interface to decrease, thereby being insufficient to maintain the current and thereby causing a rapid decrease in capacity [4].

Two approaches have recently been tried to address the above problem. One approach is to increase the electronic conductivity by adding a conductive additive, i.e., a carbon layer through the synthesis of a  $\text{LiFePO}_4/\text{C}$  composite [5-9], or by the addition of a supervalent cation-selective material [5-6]. The second approach is, controlling the particle size by optimizing the synthesis conditions [10]. It has been reported that the addition of carbon has solved the problem. The addition of carbon prior to the formation of the crystalline phase suppresses particle growth during the sintering process and increases the electronic conductivity through the contact between the particles [11].

Various carbon sources have been reported to fabricate  $\text{LiFePO}_4/\text{C}$  composites, for example, naphthalenetetracarboxylic dianhydride [12], hydroxyethylcellulose [13], resorsinol-formaldehyde gel [14], white sugar [15], black carbon [16], polypropylene [17], and sucrosa [18]. Recently, it has been reported that the residual carbon structure of the  $\text{LiFePO}_4$  particles is an important determinant of the electrochemical performance of these materials. This confirms that carbon coating with  $\text{sp}^2$  outer electron character causes relatively high electronic conduction compared to  $\text{LiFePO}_4$  particles with  $\text{sp}^3$  outer electron character, which results in increased electrochemical performance [19].

Poly(lactic acid) or polylactide (PLA) are thermoplastic aliphatic polyesters derived from renewable resources, such as corn starch (in the United States), tapioca products (yam, or starch in Asia) or sugarcane (worldwide). PLA can decompose under certain conditions, such as the presence of oxygen, and is not difficult to recycle. In this study, PLA was used as a carbon source and the heat treatment applied in preparing the  $\text{LiFePO}_4/\text{C}$  composite material was determined by TG thermogravimetric analysis.

This study reports the addition of polylactate and carbon to  $\text{LiFePO}_4$  precursors to study their effect on the behavior of  $\text{LiFePO}_4/\text{C}$  composites. A coprecipitation method was adopted to prepare  $\text{LiFePO}_4$  and its composites by addition of carbon. In order to obtain a uniform distribution of carbon, the polymer additive was dissolved in a solvent to form a solution and then homogeneously mixed with the amorphous  $\text{LiFePO}_4$  particles before the final heating step during composite synthesis.

## 2. Methods

The materials used are  $\text{LiOH}\cdot\text{H}_2\text{O}$  (Aldrich),  $(\text{NH}_4)_2\text{HPO}_4$  (Aldrich) and  $\text{FeSO}_4\cdot 7\text{H}_2\text{O}$  (Aldrich), Polylactide Acid (PLA, MW 30000) commercially purchased from Wako Japan is used without treatment.

A mixture of  $\text{LiOH}\cdot\text{H}_2\text{O}$ ,  $(\text{NH}_4)_2\text{HPO}_4$  and  $\text{FeSO}_4\cdot 7\text{H}_2\text{O}$  liquid solutions was deposited with pH control. The precipitate was then filtered, then washed with distilled water to obtain a mixture of  $\text{Fe}_3(\text{PO}_4)_2$  and  $\text{Li}_3\text{PO}_4$ . After that, stirring at high speed while nitrogen gas was flowed, the precursor obtained was then washed and filtered again.  $\text{LiFePO}_4$  cathode material was mixed with biodegradable PLA polymer at various weight ratios of 6, 8, 10, 12% polymer. Heat treatment was carried out by heating once at  $700^\circ\text{C}$  for 4 hours to obtain  $\text{LiFePO}_4$ .

The physical properties of the cathode material were analyzed using Simultaneously Thermal Analysis (STA Setaram. France), X-Ray Diffractometer (XRD Shimadzu XD 610, Japan), Scanning Electron Microscope (SEM JEOL JSM 6510, Japan), and Particle Size Analyzer (PSA). For conductivity measurement using a High Precision LCR-meter HIOKI 3532-50, China, the cathode composite was prepared by pressing  $\text{LiFePO}_4 / \text{C}$  powder with a hydraulic press of  $200\text{ kg/cm}^2$ .

## 3. Results and Discussion

This study aims to determine the effect of polymer as a carbon additive source on the electrochemical performance and physical properties of the  $\text{LiFePO}_4/\text{C}$  composite. Figure 1 shows the thermogravimetric graph (TG) and thermal analysis (DTA) of the  $\text{LiFePO}_4/\text{C}$  composite with the addition of 6% PLA.

Thermogravimetric analysis (TG) was used to determine the proper temperature in the heat treatment. The TG curve of the PLA containing precursor (Fig. 1) is typical of a powder mixture consisting of  $\text{Li}_2\text{CO}_3$ ,  $\text{FeC}_2\text{O}_4\cdot 2\text{H}_2\text{O}$ , and  $\text{NH}_4\text{H}_2\text{PO}_4$  to react to give  $\text{LiFePO}_4$  [14]. In addition, it has been previously reported [12] that the pyrolysis of PLA in a nitrogen gas stream occurs at a temperature of  $300\text{--}425^\circ\text{C}$  and that only a small amount of residue persists at temperatures up to  $450^\circ\text{C}$ . The  $\text{LiFePO}_4$  precursor with the addition of PLA contains aqueous crystals of  $\text{FeC}_2\text{O}_4\cdot 2\text{H}_2\text{O}$  and  $\text{NH}_4\text{H}_2\text{PO}_4$  which decomposes at a temperature of less than  $250^\circ\text{C}$ . In the temperature range of  $350\text{--}420^\circ\text{C}$ , there is a decrease in weight due to the decomposition of  $\text{FeC}_2\text{O}_4$  and the reaction with  $\text{NH}_4\text{H}_2\text{PO}_4$  while PLA is rapidly decomposed. After the formation of  $\text{LiFePO}_4$  at  $470^\circ\text{C}$ , the product weight decreased slightly and was very gentle.

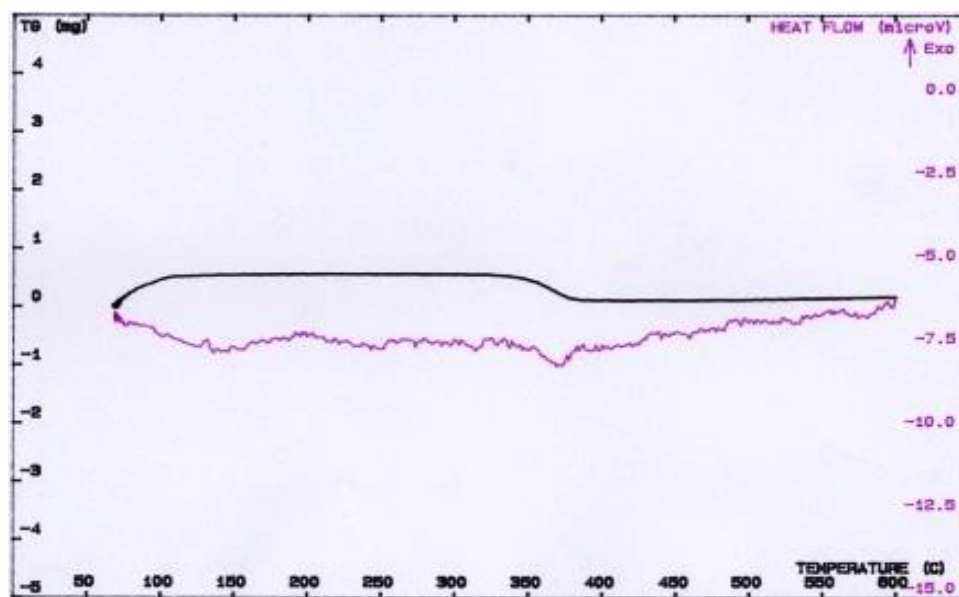


**Figure 1.** Graph of thermogravimetry (TG) and thermal analysis (DTA) of  $\text{LiFePO}_4$  / C composite with the addition of 6% PLA.

Gradual weight loss was observed above the  $\text{LiFePO}_4$  formation temperature where the pyrolysis of the remaining PLA continued up to  $600^\circ\text{C}$ . The TG pattern also showed that  $\text{LiFePO}_4$  formation and PLA pyrolysis occurred in the same temperature range. This indicates that there is a possibility of carbon coating along with the decomposition of PLA and the formation of  $\text{LiFePO}_4$  powder. There was no significant difference in the TG/DTA pattern for the addition of PLA up to 12%.

To confirm the results of the TG analysis, XRD analysis (Figure 2) was carried out on the sintered  $\text{LiFePO}_4$  powder containing 6, 8, 10 and 12% PLA, as shown in Figure 2 (a-d). Most of the samples providing XRD data are consistent with pure single-phase  $\text{LiFePO}_4$  with a slight impurity phase pattern, which is iron phosphide ( $\text{Fe}_2\text{P}$ ). The presence of  $\text{Fe}_2\text{P}$  impurities may be caused by the high carbon content combined with high temperatures causing Fe and P to form active  $\text{Fe}_2\text{P}$  [13]. The main peak of  $\text{LiFePO}_4$  diffraction occurs at an angle of  $2\theta = 17.04^\circ$ ;  $20.7^\circ$ ;  $24^\circ$ ;  $29.6^\circ$ ;  $30.98^\circ$ ;  $35.5^\circ$  and  $42.2^\circ$  correspond to crystal planes [020], [011], [101], [200], [210], [201] and [112]. While the main peak of  $\text{Fe}_2\text{P}$  occurs at an angle of  $2\theta = 25.748^\circ$ ;  $31.287^\circ$ ;  $40.317^\circ$ ;  $44.225^\circ$ ;  $47.347^\circ$  corresponds to the crystal planes [001], [101], [111], [201], [210]. Carbon C from PLA combustion has a main peak of  $2\theta = 26.403^\circ$ ;  $44.43^\circ$  and  $54.591^\circ$  correspond to the crystal planes of [002], [101] and [004].

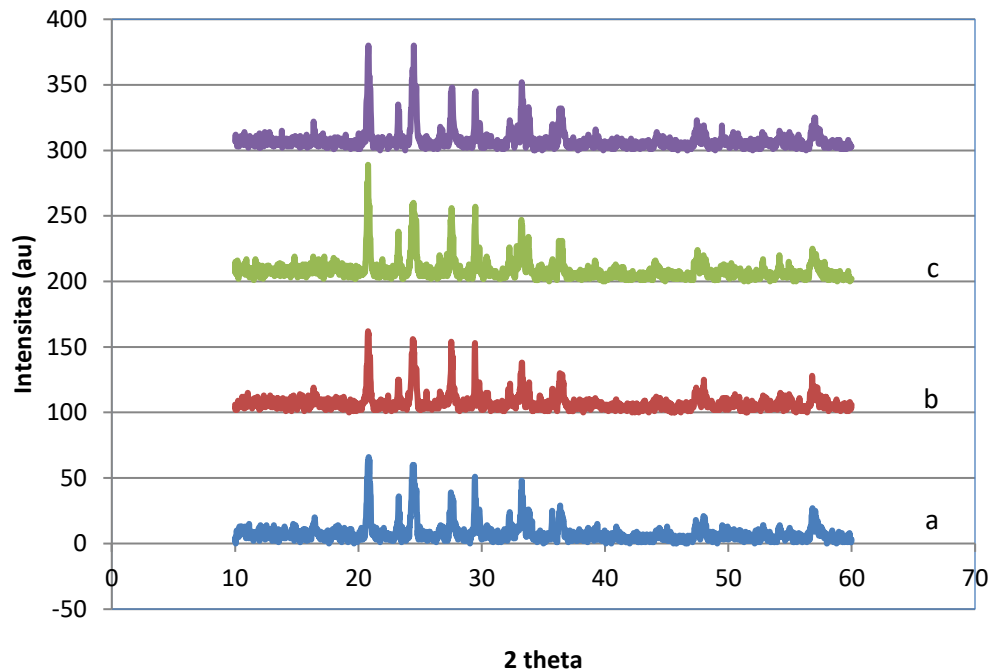


**Figure 2.** XRD pattern of sintered  $\text{LiFePO}_4$  powder with PLA content of 6% (a), 8% (b), 10% (c) and 12% (d).

The addition of different PLA content can affect the arrangement of  $\text{LiFePO}_4$  grains. The  $\text{LiFePO}_4/\text{C}$  composite is black, contrasting the gray color of  $\text{LiFePO}_4$ . This is as shown by the SEM sweep results in Figure 3. The microstructure of  $\text{LiFePO}_4$  shows that there are differences in the grain arrangement of different PLA contents. At 6% PLA content, it is clear that there is an even distribution of particles, this is because the results of the synthesis of  $\text{LiFePO}_4$  using the precipitation method so as to produce a uniform grain size (Figure 3). At higher PLA content, namely 8, 10 and 12%, the distribution of particles spreads unevenly, this is due to the inability of  $\text{LiFePO}_4$  particles to bind PLA in larger quantities. With 6% by weight of PLA in the starting material, 7.06% by weight of elemental carbon was found in the  $\text{LiFePO}_4/\text{C}$  composite at a heat treatment step of  $700^\circ\text{C}$ .

The distribution of  $\text{LiFePO}_4$  particles using volume distribution analysis from a particle size analyzer (PSA) is shown in Figure 4. From the volume distribution analysis, the average particle size is  $21.9\ \mu\text{m}$ .

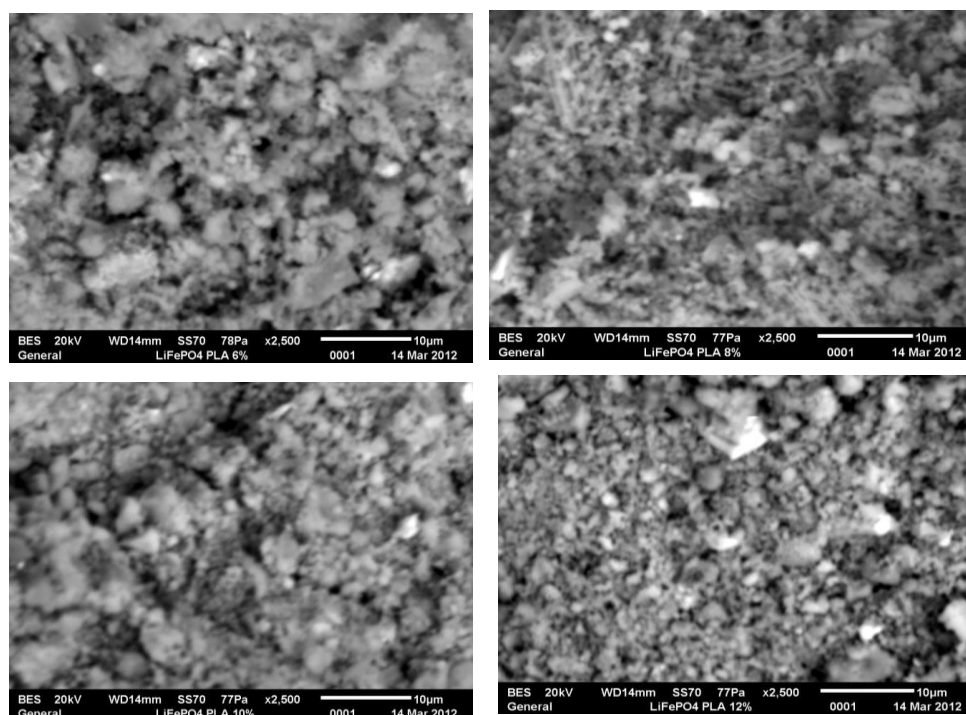


**Figure 3.** Grain arrangement of LiFePO<sub>4</sub> with different PLA content (a) 6% PLA, (b) 8% PLA, (c) 10% PLA and (d) 12% PLA.

Version 2.31 / 2.03

#### Volume Distribution

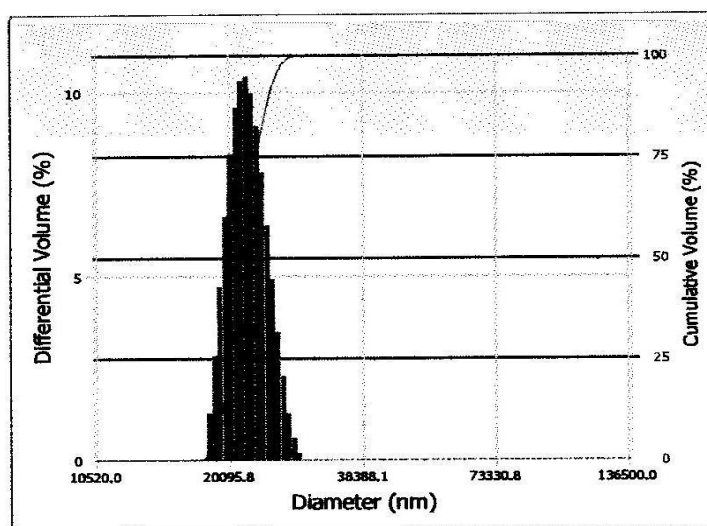


**Figure 4.** Distribution volume analysis using a particle size analyzer (PSA).

Conductivity measurements were performed using a High Precision LCR-meter connected to a computer for data acquisition. Measurements were carried out in a temperature range of 25 to 70 °C. The highest conductivity of  $1.99 \times 10^{-2} \text{ S cm}^{-1}$  was demonstrated by a LiFePO<sub>4</sub>-based cathode with a PLA concentration of 6% wt (**Figure 5**). However, the conductivity tends to decrease with



the addition of more PLA. This may be due to the limited mobility of the charge carriers and the formation of neutral ion pairs and ion aggregates.

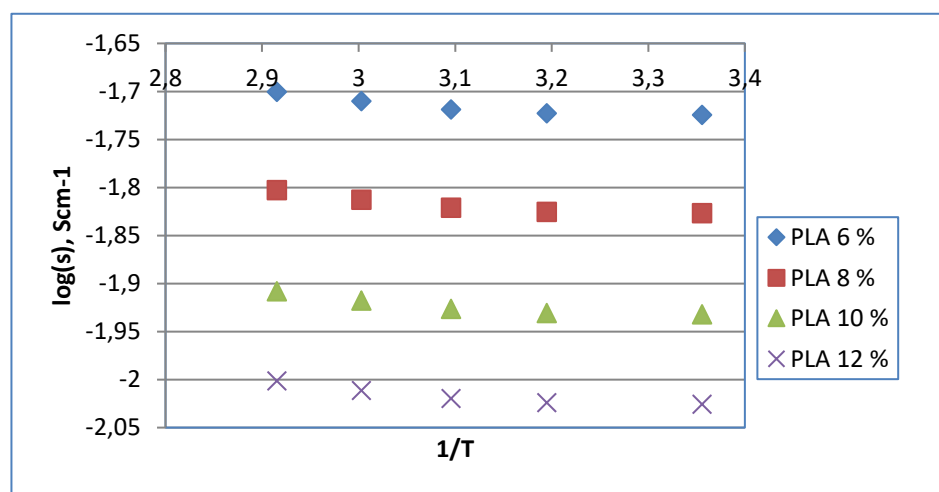


Figure 5. Graph of the log against  $1/T$  of the  $\text{LiFePO}_4/\text{PLA}$  system.

One of the important properties of a polymer electrode that must be studied is its temperature dependence on the behavior of the ionic conductivity. The graph of the log versus  $1/T$  of the system is shown in Figure 5. The graph shows the conductivity values decreasing as PLA is added. The conductivity of  $\text{LiFePO}_4$  before adding PLA was  $4 \times 10^{-4} \text{ S cm}^{-1}$  to  $1.99 \times 10^{-2} \text{ S cm}^{-1}$  on the addition of 6% PLA or an increase of almost 50 times from the initial conductivity value. The graph also shows that the conductivity increases with increasing temperature. The graph of the conductivity trend with temperature follows the empirical Vogel-Tammann-Fulcher (VTF) form, namely the migration of ions mainly on the segmental movement of the polymer chains in the amorphous region. This behavior can be explained using the free volume model. As the temperature increases, the polymer surface area increases resulting in a wider free volume. This results in increased ion mobility and segmental mobility which aids ion transport and results in an increase in conductivity.

#### 4. Conclusions

From the analysis of TG/DTA water crystals of  $\text{FeC}_2\text{O}_4 \cdot 2\text{H}_2\text{O}$  and  $\text{NH}_4\text{H}_2\text{PO}_4$  decomposed at a temperature of  $<250^\circ\text{C}$ . In the temperature range of  $350\text{--}420^\circ\text{C}$ , there was a decrease in weight due to the decomposition of  $\text{FeC}_2\text{O}_4$  and reaction with  $\text{NH}_4\text{H}_2\text{PO}_4$  while PLA quickly decomposed. Gradual weight loss was observed above the  $\text{LiFePO}_4$  formation temperature at  $470^\circ\text{C}$  where the pyrolysis of the remaining PLA continued up to  $600^\circ\text{C}$ . Most of the samples providing XRD data are consistent with single-phase pure  $\text{LiFePO}_4$  with a slight impurity phase pattern, which is iron phosphide ( $\text{Fe}_2\text{P}$ ). The microstructure of  $\text{LiFePO}_4$  shows that there are differences in the

arrangement of grains at different PLA contents. At 6% PLA content, it is clear that the distribution of particles is even and uniform. At higher PLA content, namely 8, 10 and 12%, the distribution of particles spreads unevenly, this is due to the inability of  $\text{LiFePO}_4$  particles to bind PLA in larger quantities. From the volume distribution analysis, the average particle size is 21.9  $\mu\text{m}$ . The conductivity measurements were carried out using a High Precision LCR-meter in a temperature range of 25 to 70  $^{\circ}\text{C}$ . The highest conductivity of  $1.99 \times 10^{-2} \text{ Scm}^{-1}$  was demonstrated by a  $\text{LiFePO}_4$ -based cathode with a PLA concentration of 6 wt%.

### Acknowledgement

Authors would like to thank Dr. Abu Khalid Rivai as Head of Research Center for Radiation Detection and Nuclear Analysis Technology, National Research and Innovation Agency.

### References

- [1] Marmorstein, D., Yu, T. H., Striebel, K. a, McLarnon, F. R., Hou, J., and Cairns, E. J., 2000, Electrochemical performance of lithiumsulfur cells with three different polymer electrolytes, *J. Power Sources*, 89, 219–226.
- [2] Hu, Y., Doeff, M. M., Kostecki, R., and Fiñones, R., 2004, Electrochemical performance of sol-gel synthesized  $\text{LiFePO}_4$  in lithium batteries, *J. Electrochem. Soc.*, 151 (8), A1279-1285.
- [3] Lin, Y.-C., Hidalgo, M. F. V., Chu, I.-H., Chernova, N., Whittingham, M. S., and Ong, S. P., 2017, Comparison of the Polymorphs of  $\text{VOPO}_4$  as Multi-Electron Cathodes for Rechargeable Alkali-Ion Batteries, *J. Mater. Chem. A*, 00, 1–11.
- [4] Ong, S. P., Jain, A., Hautier, G., Kang, B., and Ceder, G., 2010, Thermal stabilities of delithiated olivine  $\text{MPO}_4$  ( $\text{M} = \text{Fe}, \text{Mn}$ ) cathodes investigated using first principles calculations, *Electrochem. commun.*, 12 (3), 427–430.
- [5] Aifantis, K. E., Hackney, S. a., and Kumar, R. V., 2010, *High Energy Density Lithium Batteries*, Aifantis, K. E., Hackney, S. A., and Kumar, R. V. (Eds.) Wiley-VCH Verlag GmbH & Co. KGaA, Weinheim, Germany.
- [6] Mohan, E. H., Siddhartha, V., Gopalan, R., Rao, T. N., and Rangappa, D., 2014, Urea and sucrose assisted combustion synthesis of  $\text{LiFePO}_4 / \text{C}$  nano-powder for lithium-ion battery cathode application, *AIMS Mater. Sci.*, 1 (4), 191–201.
- [7] Cheng, L., Liang, G., El Khakani, S., and Macneil, D. D., 2013, Low cost synthesis of  $\text{LiFePO}_4/\text{C}$  cathode materials with  $\text{Fe}_2\text{O}_3$ , *J. Power Sources*, 242, 656–661.
- [8] Kaleta, A., Dłużewski, P., Wasiucionek, M., Pietrzak, T. K., Nowiński, J. L., Michalski, P. P., and Garbarczyk, J. E., 2017, TEM studies on thermally nanocrystallized vanadium-containing glassy analogs of  $\text{LiFePO}_4$  olivine, *Mater. Charact.*, 127, 214–221.
- [9] Ellis, B. L., Ramesh, T. N., Rowan-Weetaluktuk, W. N., Ryan, D. H., and Nazar, L. F.,



2012, Solvothermal synthesis of electroactive lithium iron tavorite and structure of  $\text{Li}_2\text{FePO}_4\text{F}$ , *J. Mater. Chem.*, 22 (11), 4759.

- [10] Peng, S., Li, L., Kong Yoong Lee, J., Tian, L., Srinivasan, M., Adams, S., and Ramakrishna, S., 2016, Electrospun carbon nanofibers and their hybrid composites as advanced materials for energy conversion and storage, *Nano Energy*, 22, 361–395.
- [11] Mazman, M., Cühadar, O., Uzun, D., Avci, E., Biçer, E., Kaypmaz, T. C., and Kadiröglü, Ü., 2014, Optimization of  $\text{LiFePO}_4$  synthesis by hydrothermal method, *Turkish J. Chem.*, 38 (2), 297–308.
- [12] Zhao, L., Zhao, F., and Zeng, B., 2014, Preparation and application of sunset yellow imprinted ionic liquid polymer - Ionic liquid functionalized graphene composite film coated glassy carbon electrodes, *Electrochim. Acta*, 115, 247–254.
- [13] Rajendran, S., Sivakumar, M., Subadevi, R., and Nirmala, M., 2004, Characterization of PVA-PVdF based solid polymer blend electrolytes, *Phys. B Condens. Matter*, 348 (1–4), 73–78.
- [14] Katayama, M., Sumiwaka, K., Miyahara, R., Yamashige, H., Arai, H., Uchimoto, Y., Ohta, T., Inada, Y., and Ogumi, Z., 2014, X-ray absorption fine structure imaging of inhomogeneous electrode reaction in  $\text{LiFePO}_4$  lithium-ion battery cathode, *J. Power Sources*, 269, 994–999.
- [15] Ma, J., Xue, T., and Qin, X., 2014, Sugar-derived carbon/graphene composite materials as electrodes for supercapacitors, *Electrochim. Acta*, 115, 566–572.
- [16] Huang, Y., Ying, J., and Goodenough, J., 2007,  $\text{LiFePO}_4$ /polymer composite cathodes with high rate capability, *Meet. Abstr.*, 1188 (1997), 78712.
- [17] Kim, W. S., Park, D. W., Jung, H. J., and Choi, Y. K., 2006, Suppression of co-intercalation on the carbon anode by MA addition in a PC-base electrolyte, *Bull. Korean Chem. Soc.*, 27 (1), 82–86.
- [18] Jang, S., Kim, J., Yun, Y. H., and Chung, H., 2009, Optimizing a new synthesis route for  $\text{LiFePO}_4/\text{C}$  composites, *J. Ceram. Process. Res.*, 10 (1), 95–101.
- [19] Safari, M., Farkhondeh, M., Pritzker, M., Fowler, M., Han, T., and Chen, S. K., 2014, Simulation of lithium iron phosphate lithiation/delithiation: Limitations of the core-shell model, *Electrochim. Acta*, 115, 352–357.